

## N O T I C E

THIS DOCUMENT HAS BEEN REPRODUCED FROM  
MICROFICHE. ALTHOUGH IT IS RECOGNIZED THAT  
CERTAIN PORTIONS ARE ILLEGIBLE, IT IS BEING RELEASED  
IN THE INTEREST OF MAKING AVAILABLE AS MUCH  
INFORMATION AS POSSIBLE



Technical Memorandum 80723

# Albedo, Internal Heat, and Energy Balance of Jupiter; Preliminary Results of the Voyager Infrared Investigation

R.A. Hanel, B.J. Conrath, L.W. Herath,  
V.G. Kunde and J.A. Pirraglia

SEPTEMBER 1980



National Aeronautics and  
Space Administration

**Goddard Space Flight Center**  
Greenbelt, Maryland 20771

(NASA-TM-80723) ALBEDO, INTERNAL HEAT, AND  
ENERGY BALANCE OF JUPITER, PRELIMINARY  
RESULTS OF THE VOYAGER INFRARED  
INVESTIGATION (NASA) 34 p HC A03/MF A01

N81-25013

Unclass  
25763

CSCL 03R 63/91

**ALBEDO, INTERNAL HEAT, AND ENERGY BALANCE OF JUPITER;  
PRELIMINARY RESULTS OF THE VOYAGER INFRARED INVESTIGATION**

**BY**

**R.A. HANEL, B.J. CONRATH, L.W. HERATH  
V.G. KUNDE AND J.A. PIRRAGLIA  
LABORATORY FOR EXTRATERRESTRIAL PHYSICS  
GODDARD SPACE FLIGHT CENTER  
GREENBELT, MD. 20771**

**MAY 1980**

**Revised September 1980**

**Submitted for Publication in  
Journal of Geophysical Research**

## ABSTRACT

Full disk measurements recorded 31 days before the Voyager 1 encounter with Jupiter by the radiometer (0.4-1.7  $\mu\text{m}$ ) of the infrared instrument, IRIS, indicate a geometric albedo of  $0.274 \pm 0.013$ . The given error is an estimate of systematic effects and therefore quite uncertain; the random error in the radiometer measurement is negligible. Combining this measurement with the Pioneer derived phase integral of 1.25 of Tomasko et al. (1978) and our error estimate of 0.1 yields a Jovian Bond albedo of  $0.343 \pm 0.032$ .

Infrared spectra recorded at the same time by the Michelson interferometer (4-55 $\mu\text{m}$ ), along with a model extrapolation to low wave numbers not covered by the instrument, yield a thermal emission of  $(1.359 \pm 0.014) 10^{-3} \text{ W cm}^{-2}$ . This corresponds to an equivalent blackbody temperature of  $124.4 \pm 0.3 \text{ K}$ , in agreement with results of Ingersoll et al. (1975) and Erickson et al. (1978), but lower than all other previous estimates. As in the case of the albedo measurement the quoted errors in the emission measurement reflect estimates of systematic effects and are uncertain while the random component is negligible.

From these measurements the internal heat flux of Jupiter is estimated to be  $(5.444 \pm 0.425) 10^{-4} \text{ W cm}^{-2}$ , and the energy balance defined as the ratio of emitted thermal to absorbed solar energy is  $1.668 \pm 0.085$ .

## INTRODUCTION

A precise measurement of the emitted thermal and absorbed solar energy and their ratio, generally referred to as the energy balance, is essential for achieving an understanding of the basic physical processes and structure of Jupiter. The energy balance constrains models of the interior (Smoluchowski, 1967; Hubbard, 1968, 1973; Hubbard and Smoluchowski, 1973; Graboske et al., 1975; Stevenson and Salpeter, 1976; Cameron and Pollack, 1976; Hubbard, 1980) and determines the amount of energy which must be convected vertically below the Jovian clouds. This convection has a profound effect on the physical and chemical state of the observable atmosphere.

Jupiter is known to emit more energy than it receives from the sun. The emission, mostly radiated in the infrared between 10 and 100 $\mu$ m, has been estimated from ground based measurements, airborne observations and Pioneer data, but these estimates, shown in Table 1, are not in full agreement.

The second quantity necessary for an estimate of the energy balance, the absorbed solar energy, is generally computed from a measurement of the geometric albedo, assuming a knowledge of the phase integral. Difficulties exist in establishing a good photometric calibration, and earlier albedo measurements resulted in a wide range of values. For a discussion of albedo measurements see Harris (1961), Axel (1972), and Tomasko (1976). Taylor's (1965) estimate of  $0.28 \pm 0.03$  obtained by ground based spectral photometry is currently considered the most reliable value. The phase integral has recently been estimated from Pioneer 10 data by Tomasko et al. (1978), to be between 1.2 and 1.3.

One of the objectives of the Voyager infrared investigation is to determine the energy balance of Jupiter from measurements of the reflected solar radiation with a single channel radiometer, and the spectral radiance in the infrared with a Michelson interferometer (Hanel, et al. 1977). The Voyager infrared instrument (IRIS) has been described by Hanel, et al.

(1980). The calibrations of the radiometer and the interferometer play a significant role in the accuracy of the derived energy balance; therefore, the in-flight calibration of both devices is discussed in this paper. The calibrated full disk measurements are then applied to derive values of the albedo, the thermal emission and finally the global energy balance of Jupiter.

### SELECTION OF DATA

The final evaluation of the local, zonal and total energy budget of Jupiter from the IRIS data involves a large number of observations at various latitudes and longitudes, as well as emission, phase and sun angles. Due to the nature of the fly-by trajectory, only limited coverage of the above mentioned five parameters was obtained. For example, high latitudes were not observed at low emission angles and certain ranges of the phase and sun angles which could be observed only from unique positions along the trajectory were precluded where satellite and other planetary observations were made instead. While the high spatial resolution obtained near closest approach is very valuable for other scientific objectives of the Voyager infrared investigation, the high resolution complicates the global heat balance study because local variations in brightness tend to make the precise measurement of the phase function on a planetary scale more difficult. The high resolution data set will be most useful in constraining radiative transfer models of the clouds and the atmosphere of Jupiter, but until these models can be completed a more elementary approach has been taken to obtain an estimate of the global Jovian energy balance.

At about 31 days before closest approach of Voyager 1, the apparent disk of Jupiter just filled the IRIS field of view, and the calibrations of the radiometer and the interferometer to be discussed below are directly applicable to the full disk data from that period. Effects due to the spatial structure of the clouds average out and the data can be compared to full disk measurements from the earth. During this time period, observations were selected when Jupiter was stabilized within the field of view. Maxima in the time sequence of the radiometer data were chosen on

the assumption that they indicate the best alignment of Jupiter within the IRIS field. The Digital Number (DN) of such maxima, divided by  $\omega_j/\Omega_1$  are plotted versus  $\omega_j/\Omega_1$  in Fig. 1 where  $\omega_j$  is the solid angle of Jupiter's apparent disk and  $\Omega_1$  is the solid angle of the instrument field of view. The dashed lines represent the envelope of all local maxima indicating the cases of best alignment. Images from the Voyager cameras were also used to confirm alignment. If the response of the radiometer channel were constant within the field, the dashed line would have been horizontal for values of  $\omega_j/\Omega_1$  below unity. Apparently the radiometer responsivity is slightly higher by about 12% in the center than in the average over the field. The calibration to be discussed later applies to the whole field. Second order effects caused by the small non-uniformity of the response within the field and possible longitudinal effects on Jupiter have been neglected. As expected, for cases where Jupiter is larger than the IRIS field,  $\omega_j/\Omega_1 > 1$ , the dashed curve declines sharply. The most likely value of the radiometer output for the best match between the IRIS field and the disk of Jupiter seems to be the intersection of the dashed curves yielding a Digital Number of 735.

Similar considerations for the interferometer data lead to the selection of five individual spectra for which near perfect alignment and constancy of the signal can be assumed. A significant uncertainty in the thermal emission measurement may be associated with the problem of imaging the slightly elliptical disk of Jupiter onto the circular aperture of the instrument. For four of the five spectra selected the measurements were made when the diameter of the field of view of IRIS was about equal to the polar but slightly less than the equatorial angular diameter of the planet. In the first of the five spectra the solid angle of the field was slightly larger than the solid angle of the disk. After normalizing this spectrum by the ratio of the solid angles of the field of view and the apparent disk of Jupiter, all five spectra showed nearly identical values (standard deviation 0.16%) and, therefore, the uncertainty caused by matching the image of Jupiter to the circular aperture cannot be large. The brightness temperature of the average of the five disk spectra, shown in Fig. 2, is similar to the spectra recorded at a smaller distance (Hanel et al. 1979a, 1979b), but shows, as expected, a mixture of the characteristics of spectra near the limb and near the center of the disk.

## CALIBRATION OF THE RADIOMETER

Calibration of the radiometer requires a precise knowledge of the spectral response on a radiometric scale. It is sufficient, however, to determine the spectral response in relative terms and the spectrally integrated value in absolute units.

The relative response of the radiometer was established by laboratory measurements of the reflective or transmissive properties of all components in the optical path. Either the actual components or, as in the case of curved surfaces, representative flat witness samples were measured. The samples were manufactured and coated simultaneously with the optical elements. The normalized product of all reflection and transmission functions is shown in Fig. 3. The gold coating of the primary mirror causes the roll-off at short wavelength and the coating on the dichroic mirror limits the long wavelength response.

Determination of the integrated response on an absolute scale is more difficult. The possibility of changes in the response during the launch phase and the long space journey made an in-flight calibration desirable. Two methods were used; in both the sun served as the radiation source.

The first method takes advantage of a flat aluminum plate with a bead-blasted surface. The spectral and diffusive properties of this surface were determined before launch. The spectral response in the radiometer's range of interest, 0.3 to 2 $\mu$ m, was measured with an integrating sphere (Fig. 4). Over this range and beyond to 20 $\mu$ m, the bead-blasted surface approaches a perfect diffuser. This large plate is mounted on the spacecraft and fills the field of view completely when viewed by IRIS. For calibration use, the plate is illuminated by the sun. Since this requires reorientation of the spacecraft, only a few such opportunities were provided. Such a diffuser plate calibration was performed on Feb. 9, 1979, within a few days of the measurements of Jupiter discussed in this paper. The diffuser plate calibration permitted a direct comparison of the light reflected by Jupiter to that reflected by the plate.

The power available at the radiometer detector,  $S_d$ , while viewing the plate can be expressed by

$$S_d = \frac{\omega_{ss}}{\pi} \int \pi B_{\lambda_s} d\lambda A \Omega g \bar{\tau}_d p_d \cos \beta. \quad (1)$$

The digitized signal (DN) in the spacecraft data stream is directly proportional to the power at the detector. The proportionality factor includes the nearly wavelength independent responsivity (volts/watt) of the black 18 element thermopile detector, electronic amplification and the characteristic of the analog to digital converter. The first factor on the right side in Eq. 1, the solid angle,  $\omega_{ss}$ , of the sun at the spacecraft times the integral over the solar flux ( $\pi B_{\lambda_s}$ ), is the solar constant at the spacecraft; it is followed by the area, A, solid angle,  $\Omega$ , and obscuration factor, g, of the instrument. The optical transmittance of the radiometer,  $\bar{\tau}_d$ , is calculated by weighting  $\tau$  with the solar spectrum reflected by the diffusor plate.

$$\bar{\tau}_d = \frac{\int \tau r_d B_{\lambda_s} d\lambda}{\int r_d B_{\lambda_s} d\lambda} \quad (2)$$

The albedo of the diffusor plate,  $p_d$ , is calculated from the measured spectral reflectance of the plate,  $r_d$ , weighted by the solar spectrum

$$p_d = \frac{\int r_d B_{\lambda_s} d\lambda}{\int B_{\lambda_s} d\lambda} \quad (3)$$

All integrations have been carried out from the ultraviolet to the far infrared, although only the range from 0.3 $\mu$ m to 2 $\mu$ m is significant because the radiometer transmittance is negligible outside this range. The angle  $\beta$

is the sun or illumination angle at the plate. A signal of 1160 DN was observed viewing the diffusor with a 9 DN intentional off-set measured while observing deep space. The effective signal of 1151 DN corresponds to  $1.636 \cdot 10^{-6}$  watt falling on the detector.

In the second calibration method, sunlight is reflected from a small gold-coated convex mirror mounted on the telescope (see Hanel et al, 1980, Fig 1.). A small beam enters the telescope when the optical axis is pointed in a particular direction  $20^\circ$  from the sun. However, the small solar beam has a different obscuration factor than the large beam through the whole telescope and does not illuminate the radiometer detector uniformly. Therefore, this method provides a convenient check, but it is not considered sufficiently accurate to serve as the primary calibration of the radiometer.

#### ALBEDO OF JUPITER

For Jupiter observations, the power,  $S_j$ , reaching the radiometer detector can be expressed in a form similar to Eq. 1:

$$S_j = \frac{\omega_{sj} \int_{\pi} B_{\lambda s} d\lambda}{\pi} A \Omega \tau_j p_j \phi(\alpha) \quad (4)$$

In this case,  $\omega_{sj}$  is the solid angle of the sun at Jupiter,  $\tau_j$  is the optical transmittance of the radiometer weighted by the solar spectrum reflected by Jupiter,  $p_j$  is the geometric albedo,  $\alpha$  is the phase angle and  $\phi(\alpha)$  is the phase function of Jupiter normalized to unity at  $\alpha = 0$ . The ratio  $S_j$  to  $S_d$  can be expressed by

$$\frac{S_j}{S_d} = \frac{DN_j}{DN_d} = \frac{(AU)_{sc}^2 \bar{\tau}_j p_j \phi(\alpha)}{(AU)_j^2 \bar{\tau}_d p_d \cos \beta} \quad (5)$$

As mentioned before, the DN for the Jupiter and diffusor plate measurements are 735 and 1151 respectively. The ratios of the solid angles of the sun at the spacecraft and at Jupiter have been expressed by the corresponding squares of the distances to the sun,  $(AU)_{sc}^2 = 26.2886$  and  $(AU)_j^2 = 27.8757$ , at the time of measurement. The solar radiance, telescope area, solid angle and obscuration factor cancel. The mean optical transmittances,  $\bar{\tau}$ , with respect to Jupiter ( $\bar{\tau}_j = 0.1732$ ) and the diffusor plate ( $\bar{\tau}_d = 0.1479$ ) have been computed using the laboratory transmission function shown in Fig. 3, the spectral reflectivities of Jupiter and the diffusor plate, and the spectral radiance of the sun. The spectral reflectivity of Jupiter between 0.2 and  $1\mu m$  was taken from Taylor (1965), (see also Tomasko (1976)), and between 1 and  $5\mu m$  from Ridgeway et al. (1976). The Jovian spectrum enters  $\bar{\tau}$  only in a secondary way by providing a slightly different weight to the radiometer response compared to the weight applied to the corresponding value for the diffusor. Moreover, only the relative values for  $r_j$ ,  $r_d$ , and  $B_{\lambda s}$  enter the  $\bar{\tau}$ 's. We believe that the actual radiometer transmittances are slightly lower than the quoted values, but the same factor applies to the Jupiter and diffusor measurements and therefore cancels. The albedo of the diffusor plate, 0.5018, was calculated by a numerical integration of Eq. 3. The phase function was taken as 0.9168, corresponding to that of a perfect Lambert sphere at a phase angle,  $\alpha$ , of  $24.7^\circ$  at the time of observation. The illumination angle,  $\beta$ , of the diffusor plate was  $30^\circ$ . With these numerical values applied to Eq. 5, the geometric albedo of Jupiter,  $p_j$ , is found to be 0.274.

An estimate of the probable error is very difficult because contributing uncertainties are mostly of a systematic nature. Random errors in the radiometer channel, as verified during the diffusor plate measurements, are less than one DN and are therefore negligible. To obtain an approximation of the total error, estimates of the uncertainties in the contributing quantities in Eq. 5 are made and treated as statistically independent errors. From an inspection of Fig. 1 we conclude that the DN

value of 735 is probably correct within  $\pm 10$  DN ( $\pm 1.4\%$ ). The uncertainty in the diffusor plate measurement is assumed to be, quite arbitrarily,  $\pm 5$  DN ( $\pm 0.4\%$ ) which is at least 5 times the random error in this measurement. The sun to Jupiter and sun to spacecraft distances are very well known, so no error was assigned to these quantities. The individual  $\bar{r}$  may have larger systematic errors, however; the error in the ratio was estimated to be less than  $\pm 2\%$ . The albedo of the diffusor plate is probably the least well known quantity in Eq. 4. We assign an uncertainty of  $\pm 3\%$  to the original laboratory measurements and another uncertainty of  $\pm 2\%$  to account for possible changes of the diffusor plate reflectivity in flight, including possible temperature effects. Another  $\pm 2\%$  error has been assigned to the phase function and an error of 0.5% to the precise knowledge of the illumination angle of the diffusor plate. With these assumed errors the estimated geometric albedo becomes

$$p = 0.274 \pm 0.013.$$

An estimate of the Bond albedo is obtained by multiplying the geometric albedo with the phase integral,  $q$ . Earth based data measure the phase function only up to  $12^\circ$ ; there it seems to be consistent with a phase integral of  $3/2$  expected for a Lambertian diffusor. But space borne measurements from a fly-by or, even better, from an orbiter at high inclination angle are needed to determine the phase function at all angles. For the time being we adopt the measurement of the phase integral of 1.2 to 1.3 in the red and blue channels of the Pioneer photopolarimeter by Tomasko et al. (1978). Furthermore, we assume that this value is correct for the whole spectrum of reflected sunlight and not only in the red and blue and assign an error of  $\pm 0.10$  to the total phase integral of 1.25. With the Pioneer value of the phase integral, the Bond albedo is

$$pq = 0.343 \pm 0.032.$$

In other words, approximately one third of the solar flux falling on the Jovian disk is reflected and the rest is absorbed by the atmosphere and clouds. All these quantities and their errors are summarized in Table 2.

## CALIBRATION OF THE INTERFEROMETER

In-flight calibration of the interferometer is accomplished by using deep space spectra and the precisely known temperature of the instrument. Three thermostats control the temperature of the interferometer and the telescope mirrors to a nominal  $200.0 \pm 0.1\text{K}$ . The planetary radiance,  $I_{\nu}$ , is calculated for each spectral interval from

$$I_{\nu} = \frac{C_2(\nu) - C_1(\nu)}{C_2(\nu)} B_{\nu}(T_c) \quad (6)$$

where  $C_1$  and  $C_2$  are the measured spectral amplitudes of the planetary and deep space spectra, respectively, and  $B_{\nu}(T_c)$  is the Planck function corresponding to the instrument temperature.  $C_2$  should always be larger than  $C_1$  because the net flux from the detector is at a maximum when viewing deep space. In addition to the calibrated spectral radiance of the object, the noise equivalent spectral radiance, NESR, has been computed (Hanel et al., 1980). Sequences of deep space spectra are interspersed with planetary and satellite observations. Calibration spectra are therefore available within a few hours before and after planetary observations. The calibration of planetary spectra uses a linear interpolation process between deep space spectra on both sides of a set of observations. With this procedure, long term drift in the instrument response (which was observed to be  $\sim 0.1\%$  per day at  $800\text{ cm}^{-1}$ , for example) has been eliminated, and short term drift has been minimized. Tests on individual deep space spectra imbedded in observational sequences showed that the residual background level is smaller than the NESR. While this condition holds in general, exceptions such as the following exist; however, none of these cases is used in this analysis. During sun calibrations with the small  $20^\circ$  off-axis mirror and during some phases of the near and post encounter periods the Voyager scan platform pointed near the sun and partially exposed the primary mirror to direct sunlight. The individual high-precision thermostats compensated well for the changing thermal

environment, but small temperature transients may have occurred on a short time scale. Therefore, for periods of an hour or so after a substantial slew of the platform, the absolute calibration of the spectra is probably less reliable than under the more steady state conditions.

As in the case of the radiometer measurement, random errors in the infrared radiance are small. In the nominal spectral range of the interferometer,  $200\text{--}2300\text{ cm}^{-1}$ , the effective NESR of the interferometer is about  $7 \times 10^{-9}\text{ W cm}^{-2}\text{ sr}^{-1}/\text{cm}^{-1}$ . The noise is predominantly Johnson noise from the thermopile detector, and noise in different spectral intervals is statistically independent, yielding a total noise of  $3.2 \times 10^{-7}\text{ W cm}^{-2}\text{ sr}^{-1}$  over the  $200\text{--}2300\text{ cm}^{-1}$  spectral interval. This number may be compared to the radiance from Jupiter in the same interval, about  $3.3 \times 10^{-4}\text{ W cm}^{-2}\text{ sr}^{-1}$ , corresponding to a signal to noise ratio of over 1000. The probable error in the spectrally integrated radiance due to random effects alone is therefore less than  $\pm 0.1\%$ . The standard deviation in the integrated radiance among the five spectra chosen for analysis is  $0.16\%$ , which is larger than the random error computed from the NESR. This is not surprising because some pointing uncertainty is expected to contribute variations in addition to the random noise from the detector. Since individual deep space spectra imbedded in observational sequences showed spectral radiances in the order of the NESR, we conclude that systematic errors in the internal interferometer calibration are probably less than  $0.16\%$  or  $6 \times 10^{-7}\text{ W cm}^{-2}\text{ sr}^{-1}$ . Conservatively, we adopt this radiance value also for the actual range of integration ( $230\text{--}2300\text{ cm}^{-1}$ ), although it was derived from a slightly wider spectral interval,  $175\text{--}2300\text{ cm}^{-1}$ . However, as in the case of the radiometer, the effect of non-uniformities within the field of view has been neglected. To account for unknown uncertainties in the mismatch between the elliptical image of Jupiter and the circular aperture, a possible uncertainty of 5 times the standard deviation in the set of five spectra was arbitrarily assigned.

Another systematic error source of instrumental nature is in the calibration of the temperature sensor used to derive the instrument temperature. The temperature at several locations within the instrument is monitored before and after each interferogram. For the calibration a

temperature reading near the interferometer detector is used. The bead thermistor, epoxied into a small hole in the beryllium structure, was chosen for its long term stability (drift less than 0.1K in eight years). The thermistor was calibrated by the National Bureau of Standards. The precision of the digital readout is 0.0038K per digital number. It is estimated that the absolute error in the temperature reading is less than  $\pm 0.1\text{K}$ . In this case  $\sigma T_1^4$ , where  $T_1$  is the instrument temperature, is known to better than  $\pm 0.2\%$ .

### EXTRAPOLATION TO LOW WAVENUMBERS AND DETERMINATION OF THE THERMAL EMISSION OF JUPITER

The IRIS spectrum covers the range from about 200 to 2500  $\text{cm}^{-1}$ , but a significant fraction of the Jovian emission is below 200  $\text{cm}^{-1}$ . To obtain a reliable estimate of this fraction, a radiative transfer model was used. First, the vertical temperature profile was deduced from the average of the 5 spectra discussed above, assuming a mean emission angle of  $48^\circ$ , the emission angle most representative for flux calculations according to the first Eddington approximation, see e.g. Wolley and Stibbs, 1953. The derived temperature profile indicated a temperature minimum of about 107 K at 150 mb and was similar to the profiles derived subsequently from spectra obtained at higher spatial resolution. Second, this temperature profile was used with absorption by molecular hydrogen, helium, ammonia and a haze to calculate the thermal emission spectrum below 300  $\text{cm}^{-1}$  with a line by line molecular absorption program. The haze was modeled as a gray absorber with its base at 0.7 bar where ammonia saturation begins, and a scale height of 3 km which approximates the saturation curve (Goorvitch et al., 1979). The total optical depth of the haze and the ammonia concentration were left as free parameters for matching the model spectrum to the observed spectrum in the 200 to 300  $\text{cm}^{-1}$  range. While this empirical procedure is adequate for the intended use in extrapolating the spectrum to low wavenumbers, the average disk spectrum is not well suited to derive cloud or ammonia concentrations. Spectra from homogeneous regions and at constant emission angles must be used for that purpose. However, this empirical technique produced an emission spectrum which matches the overlap region well, as shown in Fig. 5.

The final spectral integration necessary to derive the Jovian flux was then carried out using the model spectrum up to  $230 \text{ cm}^{-1}$  and the measured spectrum between 230 and  $2300 \text{ cm}^{-1}$ . Above  $2300 \text{ cm}^{-1}$ , thermal emission from Jupiter is negligible. The spectral integration yielded a radiance of  $(4.326 \pm 0.043) 10^{-4} \text{ W cm}^{-2} \text{ sr}^{-1}$ , averaged over the whole disk. Finally, the Jovian flux is calculated to be  $(1.359 \pm 0.014) 10^{-3} \text{ W cm}^{-2}$ . This flux corresponds to an equivalent blackbody temperature of  $124.4 \pm 0.3 \text{ K}$ . The errors included are the estimated instrumental and imaging error of the interferometer, 0.16% and ~~0.8%~~<sup>1.06%</sup> respectively, a possible error of 2% assigned to the uncertainty in the model calculations at low wave numbers and a 0.2% error due to the calibration of the temperature transducer. In summations the actual error quantities, and in multiplications the percentage errors have been combined. All quantities and errors related to the interferometer measurement are summarized in Table 3.

In the flux calculation derived from the measured intensity, several tacit assumptions have been made. To examine the assumptions we consider the definition of the spectral flux, (Chandrasekhar, 1949):

$$\pi F_{\nu} = \int I_{\nu}(\delta, \varphi) \cos \delta \, d\omega \quad (6) \quad 7$$

where  $\delta$  is the emission,  $\varphi$  the azimuthal and  $\omega$  the solid angle. Even in a real atmosphere it is generally valid to assume that the spectral radiance,  $I_{\nu}$ , describing thermal emission depends only on  $\delta$  and not on  $\varphi$ . Special cases such as may occur at the edges of clouds may play a role in the local heat balance but are not expected to be significant on a global scale. Therefore, the flux equation can be simplified to the form

$$\pi F_{\nu} = 2\pi \int I_{\nu}(\delta) \cos \delta \sin \delta \, d\delta \quad (7) \quad 5$$

where  $I_{\nu}$  depends only on  $\delta$ . Therefore, an estimate of the global flux would require radiance measurements as a function of  $\delta$  for all surface elements and subsequently integration over  $\delta$  and the whole globe. However, if one assumes that the  $\delta$  dependence of  $I_{\nu}$  is everywhere the same, the integration over all emission angles and the globe can be accomplished by a

measurement of the radiance averaged over the whole disk from a great distance. The applicable equation is formally identical to Eq. 7; in this case  $\delta$  is the emission angle with respect to the Jupiter spacecraft line. In all cases integration over wave numbers must also be accomplished. This concept is the basis of our flux determination. How valid is the assumption of uniformity with respect to the  $\delta$  dependence? An inspection of a large number of IRIS spectra has shown a high degree of similarity in the overall spectral characteristics, and  $\delta$  dependence, even between such diverse areas as belts and zones. The greatest variation in the radiances is seen at  $2000 \text{ cm}^{-1}$  in the "hot spot" region of the planet. A more serious problem concerns the thermal emission from the polar regions which are poorly viewed from the Voyager trajectory. IRIS observations indicate, for example, a small asymmetry between the emissions of north and south high latitude regions (Hanel et al., 1979a, 1979b). Although these and other local variations do exist they are not expected to affect the global heat balance as discussed in this paper in a substantial way. Furthermore, Pioneer data (Ingersoll et al., 1975) have shown that the latitudinal variation in thermal emission of Jupiter is relatively small. In particular the high latitude approach of Pioneer 11 allowed good polar measurements. Therefore, the determination of the total flux from a disk measurement seems to be an acceptable procedure. Possible errors in the derived flux due to the non-uniformity of the Jovian emission can be estimated better after the large quantity of IRIS spectra are analyzed. For the time being we accept the disk measurement as a good approximation to the total Jovian flux.

### ENERGY BALANCE

Assuming a solar constant at one Astronomical Unit of  $0.1374 \pm 0.0007 \text{ W cm}^{-2}$  (Willson et al., 1980), and a mean orbital radius of 5.203 AU, the solar constant at Jupiter's mean distance is  $(5.076 \pm 0.025) 10^{-3} \text{ W cm}^{-2}$ . The heat balance calculations are based on the mean orbital radius of Jupiter, although Jupiter was at 5.2797 AU at the time of observation and moving towards perihelion. In terms of time Jupiter was at the mean orbital radius of 5.203 AU approximately 7 months before the Voyager

observations took place. With a radiative time constant of approximately one year (Gierasch and Goody, 1969) corresponding to the 400 mb level appropriate to the effective Jovian temperature of 124.4K, the thermal state of Jupiter at the time of our observations should be fairly well represented by calculations using the mean orbital radius. Moreover, calculations regarding the energy balance and the internal heat should be referred to the mean orbital radius rather than to the instantaneous radius at the time of measurement. It is possible that the Jovian albedo and the thermal emission depend somewhat on the orbital position of Jupiter. However, the Voyager mission, even with the 4 month time difference between arrival of the two spacecraft, is not expected to provide experimental evidence for such dependence. In this paper we have neglected this possible relationship of the albedo and thermal emission to the orbital radius and have calculated the energy balance for the mean orbital position of Jupiter using the measured albedo and emission data. With a Bond albedo of  $0.343 \pm 0.032$ , Jupiter absorbs  $(3.335 \pm 0.165) 10^{-3} \text{ W cm}^{-2}$  averaged over the exposed cross section or a total of  $(5.014 \pm 0.248) 10^{17} \text{ W}$ . The average thermal emission of  $(1.359 \pm 0.014) 10^{-3} \text{ W cm}^{-2}$  corresponds to a total emission of  $(8.365 \pm 0.084) 10^{17} \text{ W}$  and is therefore about  $1.668 \pm 0.085$  times as large as the energy received from the sun. In the calculations of the Jovian cross section and surface area, an equatorial radius of 71541 km and a polar radius of 66896 km have been assumed (Lindal et al., 1981). Jupiter's excess power output is  $(3.351 \pm 0.262) 10^{17} \text{ W}$ . Relative to the solar luminosity, the Jovian luminosity is given by  $\log(L_J/L_S) = -9.062$ . The quantities used to calculate the energy balance are summarized in Table 4.

## DISCUSSION

The energy balance derived in this paper,  $\sim 1.67$ , is at the low end of the range of previously accepted values which range from 1.6 to approximately 2.5. Our measurement of the infrared emission ( $T_e = 124.4 \pm 0.3\text{K}$ ) is in agreement with the Pioneer results ( $T_e = 125 \pm 3\text{K}$ ) and the measurement of Erickson et al. ( $T_e = 123 \pm 2\text{K}$ ) but lower than all other previous ground based and air borne measurements. Our measurement of the

geometric albedo,  $0.274 \pm 0.013$ , is slightly lower but close to and certainly consistent with Taylor's value of  $0.28 \pm 0.028$ . In our energy balance estimate we accepted a value of  $1.25 \pm 0.10$  for the phase integral (Tomasko et al. 1978) derived from data of the Pioneer photopolarimeter and our own error estimate. If we would have assumed a phase integral of 1.5, the value expected from a Lambertian sphere, the energy balance value would increase from 1.67 to 2.00.

The components of the energy balance are shown in Fig. 6. The spectral flux in  $W\text{ cm}^{-2}/\log v$  is plotted versus wave number on a logarithmic scale. Areas under the curves are therefore in  $W\text{ cm}^{-2}$  and can be compared to each other. Between 230 and 2300  $\text{cm}^{-1}$  the average of the 5 measured spectra is shown. Below 230  $\text{cm}^{-1}$ , the calculated spectrum is based on the discussed radiative transfer model. Above 3000  $\text{cm}^{-1}$ , the upper curve represents the spectral solar flux at Jupiter divided by the geometry factor of 4.0938 to account for the surface to cross section ratio of the Jovian ellipsoid. The lower curve indicates the reflected solar radiation adjusted to the radiometer measurement and a phase integral of 1.25.

Some authors use only the standard deviation in their measurement as the basis of calculating error bars. This procedure is justified where the random errors are large compared to systematic effects. As discussed above, however, the strictly random errors in the IRIS data are very small and in this sense the Voyager measurements represent significant progress. However, to quote only the random errors would be misleading since the overall accuracy of the measurement is limited by systematic effects rather than by random noise. For that reason we have tried to include estimates of the magnitude of various possible systematic effects and have combined them assuming statistical independence, while fully realizing the objections to this approach. We hope, however, that this procedure has led to a more realistic assessment of the overall accuracy of the derived quantities than a quotation of only the small random errors would have provided.

One may wonder why the error bars assigned to the interferometer measurement are much smaller than those assigned to the radiometer data. There are several reasons. First, the interferometer measures the detailed structure of the spectrum, while in the case of the radiometer the spectral characteristics of Jupiter and the instrument must be derived from ground based and laboratory measurements. Only data from a radiometer with a perfectly flat response over the whole spectral range can be interpreted without "a priori" knowledge of the spectral characteristics of the object under investigation. Second, the calibration sources used for the interferometric measurement, deep space and the internal temperature of the IRIS, are well defined, while considerable uncertainties exist in the properties of the diffusor plate which is the calibration source for the radiometer. Finally, measurements of the reflected radiation are inherently more difficult because of the role of the phase effect compared to the essentially phase-independent thermal emission measurements.

Before the IRIS interpretation can be considered complete in this area, phase functions must be derived and the heat balance on zonal and local scales must be determined. The local energy balance promises to give a better insight into the Jovian dynamics. As mentioned in the introduction, the globally averaged internal energy flux is one of the significant boundary conditions which models of the interior of Jupiter must satisfy. The agreement between the measured internal power and the power predicted by the model of Graboske et al. (1975) suggests that gravitational and internal energies of Jupiter are quite adequate to explain the present magnitude of the observed internal heat flux. Therefore, additional energy sources such as may be provided by the phase separation of helium and hydrogen in the deep interior of Jupiter (Salpeter, 1973) are probably not significant. Other important constraints on models of the interior, also derived from IRIS data, are the volume concentration of helium,  $0.103 \pm 0.030$  (Gautier et al., 1980) and the temperature at the pressure level below which an adiabatic lapse rate can be assumed; present estimates yield 136 K at 500 mb for these quantities.

#### ACKNOWLEDGEMENT

We thank J. Pearl for critically reading the manuscript.

## References

- Armstrong, K.R., D.A. Harper, Jr., and F.J. Low, Far-infrared temperature of the planets, *Ap. J.*, 178, L89-L92, 1972.
- Aumann, H.H., and C.M. Gillespie, Jr., The internal powers and effective temperatures of Jupiter and Saturn, *Ap. J.*, 157, L69-L72, 1969.
- Axel, L., Inhomogeneous models of the atmosphere of Jupiter, *Ap. J.* 173, 451-468, 1972.
- Cameron, A.G.W. and J.B. Pollack, On the origin of the solar system and of Jupiter and its satellites, Jupiter edited by T. Gehrels, pp 61-84, Univ. of Arizona Press, Tucson, 1976.
- Chandrasekher, S., Radiative Transfer, Oxford University Press, Oxford, England, 1950.
- Chase, S.C., R.D. Ruiz, G. Munch, G. Neugebauer, M. Schroeder, and L.M. Trafton, Pioneer 10 infrared radiometer experiment: preliminary results, *Science*, 183, 315-317, 1974.
- Erickson, E.F., D. Goorvitch, J.P. Simpson, and D.W. Stecker, Far infrared brightness temperature of Jupiter and Saturn, Icarus, 35, 61-73, 1978.
- Goorvitch, D., E.F. Erickson, J.P. Simpson, and A.T. Tokunaga, The mean Jovian temperature structure derived from spectral observations from 105 to  $630\text{ cm}^{-1}$ , Icarus, 40, 75-86, 1979.
- Gautier, D., B. Conrath, M. Flasar, R. Hanel, V. Kunde, A. Chedin and N. Scott, The helium abundance on Jupiter from Voyager, this issue.
- Gierasch, P. J., and R. M. Goody, Radiative time constants in the atmosphere of Jupiter, *J. Atmospheric Sciences*, 26, 979-980, 1969.
- Graboske, H.C., Jr., J.B. Pollack, A.S. Grossman and R.J. Olness, The structure and evolution of Jupiter, the fluid contraction phase, *Ap. J.* 199, 265-281, 1975.
- Hanel, R., B. Conrath, D. Gautier, P. Gierasch, S. Kumar, V. Kunde, P. Lowman, W. Maguire, J. Pearl, J. Pirraglia, C. Ponnampereuma, and R. Samuelson, The Voyager infrared spectroscopy and radiometry investigation, *Space Science Reviews* 21, 129-157, 1977.

- Hanel, R., B. Conrath, M. Flasar, V. Kunde, P. Lowman, W. Maguire, J. Pearl, J. Pirraglia, R. Samuelson, D. Gautier, P. Gierasch, S. Kumar, and C. Ponnampereuma, Infrared Observations of the Jovian System from Voyager 1, *Science*, 204, 972-976, 1979a.
- Hanel, R., B. Conrath, M. Flasar, L. Herath, V. Kunde, P. Lowman, W. Maguire, J. Pearl, J. Pirraglia, R. Samuelson, D. Gautier, P. Gierasch, L. Horn, S. Kumar and C. Ponnampereuma, Infrared Observations of the Jovian System from Voyager 2, *Science* 206, 952-956, 1979b.
- Hanel, R., D. Crosby, L. Herath, D. Vanous, D. Collins, H. Creswick, C. Harris, and M. Rhodes, Infrared Spectrometer for Voyager, *Appl. Optics*, 19, 1391-1400, 1980.
- Harris, D.L., Photometry and polarimetry of planets and satellites, Planets and Satellites G.P. Kuiper and B.M. Middlehurst, eds. pp. 272-342 Chicago, Illinois, University of Chicago Press, 1961.
- Hubbard, W.B., Thermal structure of Jupiter, *Ap. J.* 152, 745-754, 1968.
- Hubbard, W.B., Observational constraint on the structure of hydrogen planets, *Ap. J.* 182, L35-38, 1973.
- Hubbard, W. B., Intrinsic Luminosities of the Jovian Planets, *Reviews of Geophys. and Space Physics*, 18, No 1, 1-9, 1980.
- Hubbard, W.B. and R. Smoluchowski, Structure of Jupiter and Saturn, *Space Science Rev.*, 14, 599-662, 1973.
- Ingersoll, A.D., G. Munch, G. Neugebauer, D.J. Diner, G.S. Orton, B. Schupler, M. Schroeder, S.C. Chase, R.D. Ruiz and L.M. Trafton, Pioneer 11 infrared radiometer experiment: the global heat balance of Jupiter, *Science*, 188, 472-473, 1975.
- Ingersoll, A.P., G. Munch, G. Neugebauer, and G.S. Orton, Results of the infrared radiometer experiment on Pioneer 10 and 11, Jupiter edited by T. Gehrels pp. 197-215, Univ. of Arizona Press, Tucson, 1976.
- Kunde, V., D. Gautier, W. Maguire, R. Hanel, A. Marten, J.P. Fallulean, D. Rowan, A. Chedin, N. Scott, and N. Husson, Atmospheric composition of Jupiter from the infrared spectroscopy experiment on Voyager, In preparation.

- Lindal, G.F., G. E. Wood, G. S. Levy, J. D. Anderson, D. N. Sweetman, H.B. Hotz, B. J. Buckles, D. P. Holmes, P. E. Doms, V. R. Eshleman, G. E. Tyler, and T. A. Croft, The atmosphere of Jupiter: An analysis of the Voyager radio occultation measurements, this issue.
- Low, F.J., Planetary radiation at infrared and millimeter wavelength, Lowell Obs. Bull. 128 (No. 9) pp 184-187, 1965.
- Menzel, D.H., W.W. Coblentz, and C.O. Lampland, Planetary temperatures derived from water-cell transmissions, Ap. J. 63, pp 177-187, 1926.
- Murphy, R.E., and R.A. Fesen, Spatial variations in the Jovian 20-micrometer flux, Icarus, 21, 42-46, 1974.
- Murray, B.C. and R.L. Wildey, Stellar and planetary observations at 10 microns, Ap. J. 137, 692-693, 1963.
- Orton, G.S., The thermal structure of Jupiter, 1. Implications of Pioneer 10 infrared radiometer data, Icarus, 26, 125-141, 1975.
- Ridgway, S.T., H.P. Larson, and U. Fink, The infrared spectrum of Jupiter, Jupiter edited by T. Gehrels pp 384-417, Univ. of Arizona Press, Tucson, 1976.
- Salpeter, E., On convection and gravitational layering in Jupiter and in stars of low mass, Astrophysical J., 181, L83-L86, 1973.
- Smoluchowski, R., Internal structure and energy emission of Jupiter, Nature 215, 691-695, 1967.
- Stevenson, D.J. and E.E. Salpeter, Interior models of Jupiter, Jupiter edited by T. Gehrels, pp 85-112, Univ. of Arizona Press, Tucson, 1976.
- Taylor, D.J., Spectrophotometry of Jupiter's 34100-1000 Å spectrum and a bolometric albedo for Jupiter, Icarus, 4, 362-373, 1965.
- Tomasko, M.G., Photometry and Polarimetry of Jupiter, Jupiter edited by T. Gehrels, pp 486-515, Univ. of Arizona Press, Tucson, 1976.
- Tomasko, M.G., R.A. West, and N.D. Castillo, Photometry and polarimetry of Jupiter at large phase angles, Icarus 33, 558-592, 1978.
- Trafton, L., and R. Wildey, Jupiter: a comment on the 8 to 14 micron limb darkening, Ap. J., 194, 499-502, 1974.
- Wildey, R.L., Structure of the Jovian disk in the  $\nu_2$ -band of ammonia at 10000 Å, Ap. J. 154, 761-770, 1968.
- Willson, R.C., C.H. Duncan, and J. Geist, Direct measurement of solar luminosity variation, Science 207, 177-179, 1980.
- Wolfe, R. v. d. R., and D. W. N. Stibbs, The outer layers of a star, Oxford at the Clarendon Press, 1953.

Table 1  
Measurements of the Thermal Emission of Jupiter

Author	Year	T (K)	Energy Balance	Type of Measurement
Menzel et al.	1926	130 ± 10		Ground based
Murray and Wildey	1963	128 ± 2.3		Ground based
Low	1965	132 ± 6 at 10μm 127 ± 6 at 20μm		Ground based Ground based
Aumann et al.	1969	134 ± 4	2.5 ± 0.5	Aircraft
Armstrong et al.	1972	134 ± 4	2.5 ± 0.5	Aircraft
Trafton and Wildey	1974	135 ± 4		Ground based
Mu. phy and Fesen	1974	136 ± 5		Ground based
Ingersoll et al.	1976	125 ± 3	1.9 ± 0.2	Pioneer spacecraft
Erickson et al.	1978	123 ± 2	1.6 ± 0.2	Aircraft
This work	1981	124.4 ± 0.3	1.668 ± 0.085	Voyager Spacecraft

$T_e$  represents the equivalent blackbody temperature.

**Table 2**  
**Summary of Radiometer Measurement**

Quantity	Numerical Value and Uncertainty	Probable Error in %
Jupiter disk measurement	735 ± 10 DN	±1.4
Diffusor plate calibration in space	1151 ± 5 DN	±0.4
Diffusor plate reflectivity measurement before launch	0.502 ± 0.015	±3
Possible changes in diffusor plate reflectivity in space	0.502 ± 0.01	±2
Ratio of optical transmission of radiometer, $\tau_j/\tau_d$	1.172 ± 0.023	±2
Normalized phase function of Jupiter at 24.7°	0.917 ± 0.018	±2
Cosine of illumination angle of diffusor plate	0.866 ± 0.004	±.5
Geometric albedo of Jupiter	0.274 ± 0.013	±4.8
Phase integral	1.25 ± 0.10	±8
Bond albedo of Jupiter	0.343 ± 0.032	±9.3

**Table 3**  
**Summary of Interferometer Measurement**

Quantity	Numerical Value and Uncertainty	Probable Error in %
Average integrated radiance of 5 disk spectra between 175 and 2300 $\text{cm}^{-1}$ and standard deviation.	$(3.482 \pm 0.006) 10^{-4} \text{ W cm}^{-2} \text{ sr}^{-1}$	$\pm 0.16$
Same spectra between 230 and 2300 $\text{cm}^{-1}$	$(2.819 \pm 0.006) 10^{-4} \text{ W cm}^{-2} \text{ sr}^{-1}$	$\pm 0.21$
Possible error due to shape of Jupiter image, 5 times standard deviation	$(2.819 \pm 0.030) 10^{-4} \text{ W cm}^{-2} \text{ sr}^{-1}$	$\pm 1.06$
Model calculation and error in extrapolation to low wavenumbers, 2% of radiance up to 230 $\text{cm}^{-1}$	$(1.507 \pm 0.030) 10^{-4} \text{ W cm}^{-2} \text{ sr}^{-1}$	$\pm 2.0$
Total radiance (0-2300 $\text{cm}^{-1}$ )	$(4.326 \pm 0.043) 10^{-4} \text{ W cm}^{-2} \text{ sr}^{-1}$	$\pm 1.0$
Possible error due to temperature sensor in instrument		$\pm 0.2$
Thermal flux (0-2300 $\text{cm}^{-1}$ )	$(1.359 \pm 0.014) 10^{-3} \text{ W cm}^{-2}$	$\pm 1.0$
Equivalent blackbody temperature	$124.4 \pm 0.3\text{K}$	

**Table 4**  
**Summary of Energy Balance Quantities**

Quantity	Numerical Value and Uncertainty	Probable Error in %
Bond albedo	$0.343 \pm 0.032$	$\pm 9.3$
Solar constant at Earth	$0.1374 \pm 0.0007$	$\pm 0.5$
Solar constant at Jupiter's mean distance, 5.203 A.U.	$(5.076 \pm 0.025) 10^{-3} \text{ W cm}^{-2}$	$\pm 0.5$
Reflected solar energy	$(1.741 \pm 0.163) 10^{-3} \text{ W cm}^{-2}$	$\pm 9.4$
Absorbed solar energy	$(3.335 \pm .165) 10^{-3} \text{ W cm}^{-2}$	$\pm 4.9$
Total solar energy absorbed by Jovian disk, cross section $\approx 1.5035 10^{20} \text{ cm}^2$	$(5.014 \pm 0.248) 10^{17} \text{ W}$	$\pm 4.9$
Thermal emission	$(1.359 \pm 0.014) 10^{-3} \text{ W cm}^{-2}$	$\pm 1.0$
Total thermal energy emitted by Jovian ellipsoid, surface area $\approx 6.1551 10^{20} \text{ cm}^2$	$(8.365 \pm 0.084) 10^{17} \text{ W}$	$\pm 1.0$
Total internal heat source	$(3.351 \pm 0.262) 10^{17} \text{ W}$	$\pm 7.8$
Internal heat flux	$(5.444 \pm 0.425) 10^{-4} \text{ W cm}^{-2}$	$\pm 7.8$
Energy balance, total emitted/absorbed solar energy	$1.668 \pm 0.085$	$\pm 5.1$

## Figure Captions

- Fig. 1. Maxima of radiometer data divided by the ratio of the solid angle of Jupiter,  $\omega_j$ , to the IRIS field of view,  $\omega_i$ , as a function of this ratio. The intersection of the dashed lines represents near optimum alignment between the image of Jupiter and IRIS.
- Fig. 2. Brightness temperature of the average of 5 Jovian disk spectra. One spectrum was scaled to the ratio of solid angles of Jupiter and the instrument, the other 4 spectra correspond to cases where Jupiter's polar axis is close to the IRIS FOV, but the equatorial axis is slightly larger.
- Fig. 3. Spectral transmission of the IRIS radiometer shown as a function of wavelength. The fraction of the total solar flux below the corresponding wavelength is also shown. The wavelength scale is non-linear.
- Fig. 4. Spectral reflectivity of the diffusor plate versus wavelength. Also included is a scale showing the fraction of the total solar flux below the corresponding wavelength.
- Fig. 5. Brightness temperature of measured Jovian disk spectrum (solid line) and low wavenumber extension of spectrum calculated with a radiative transfer model (dotted line). Between 200 and 300  $\text{cm}^{-1}$  the agreement between both curves is within the width of the plotted lines.
- Fig. 6. Energy balance of Jupiter. The thermal emission between 230 and 2300  $\text{cm}^{-1}$  is the average of 5 disk spectra measured by IRIS; below 230  $\text{cm}^{-1}$  the emission is derived by model calculations constrained to match the measured spectrum between 200 and 300  $\text{cm}^{-1}$ . The reflected solar spectrum (lower curve above 3000  $\text{cm}^{-1}$ ) was calculated from the solar spectrum at the distance of Jupiter (upper curve) and a Bond albedo of 0.343. The detailed structure in the reflection spectrum is from ground based measurements (Taylor, 1965).

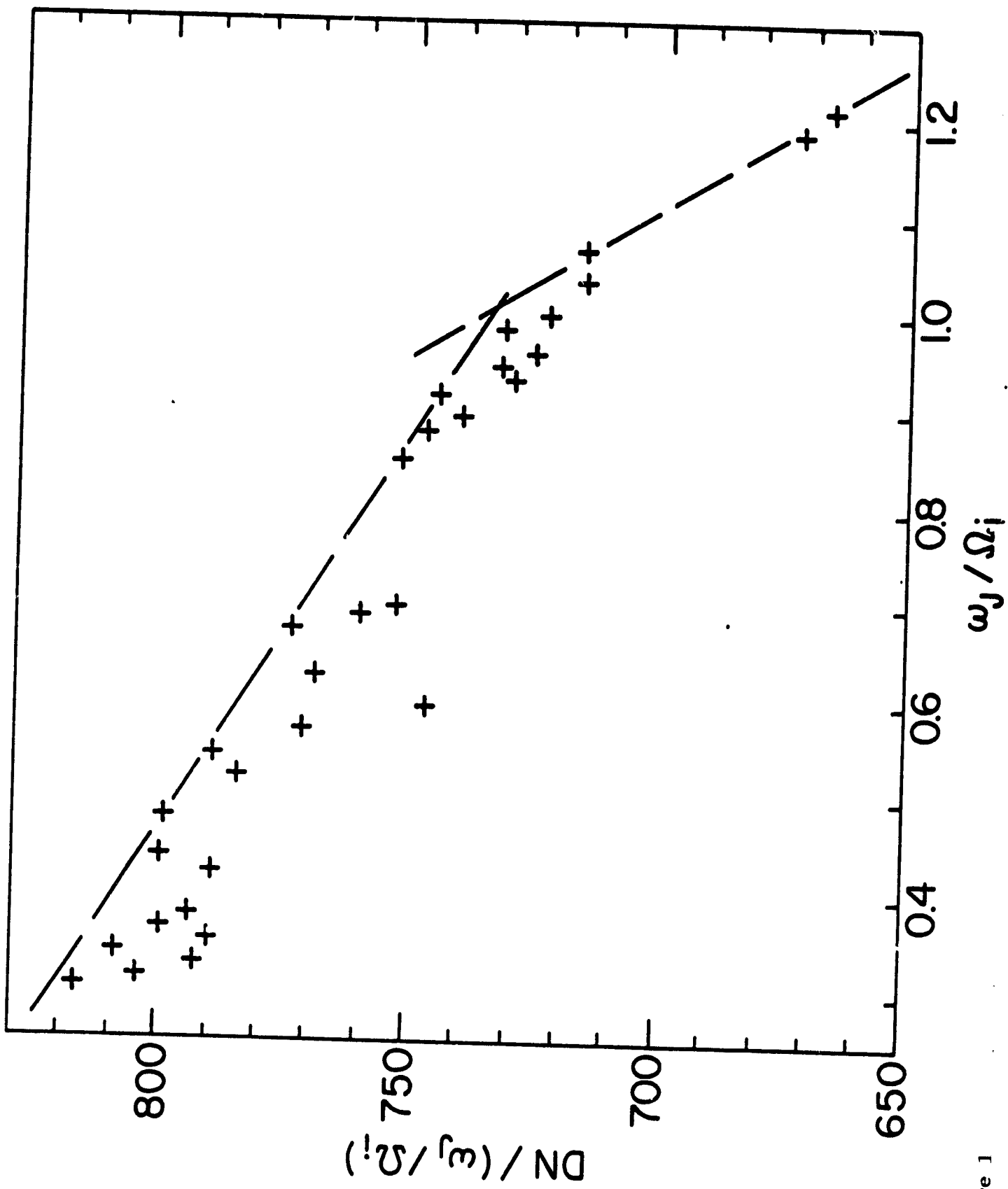


Figure 1

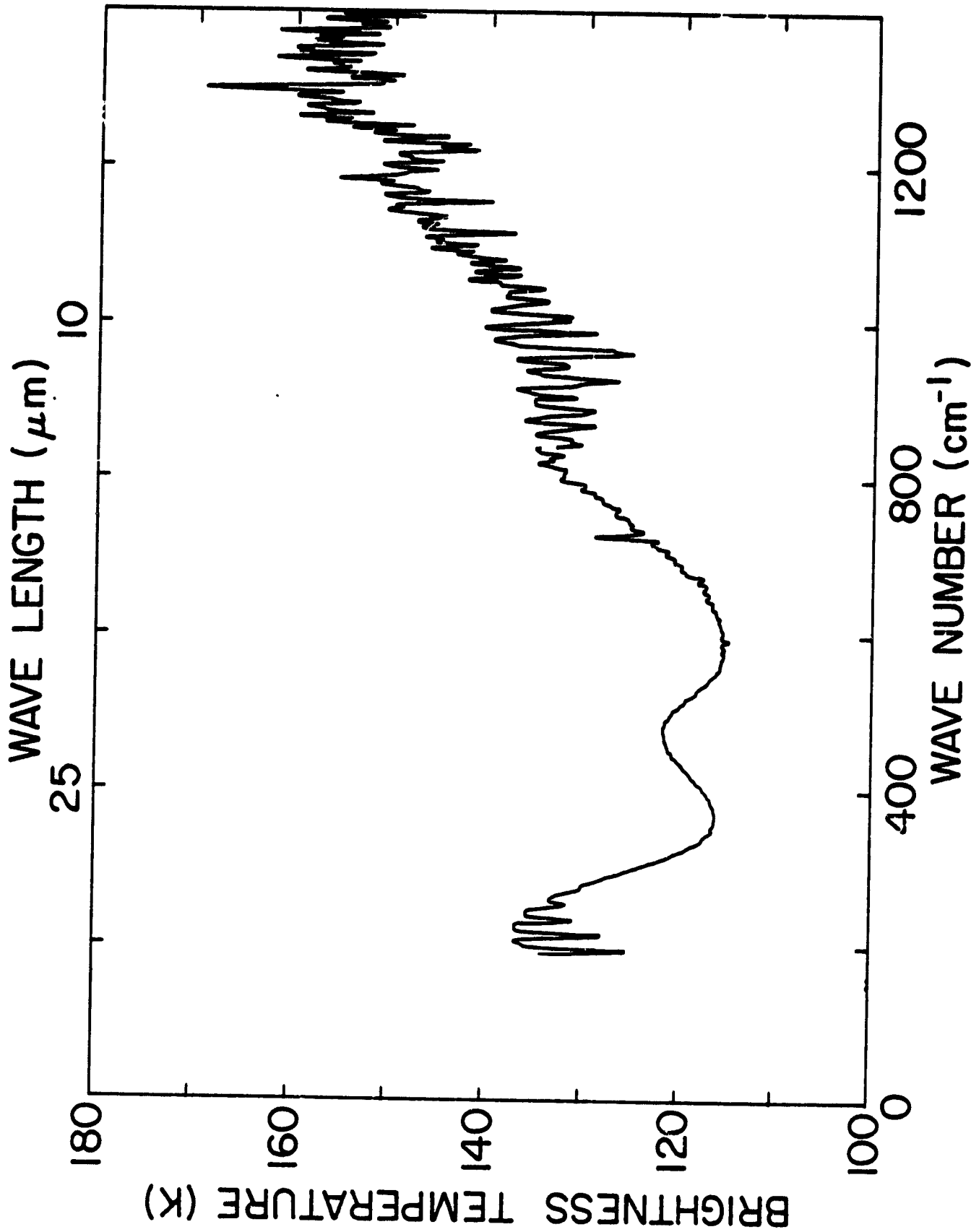


FIGURE 2

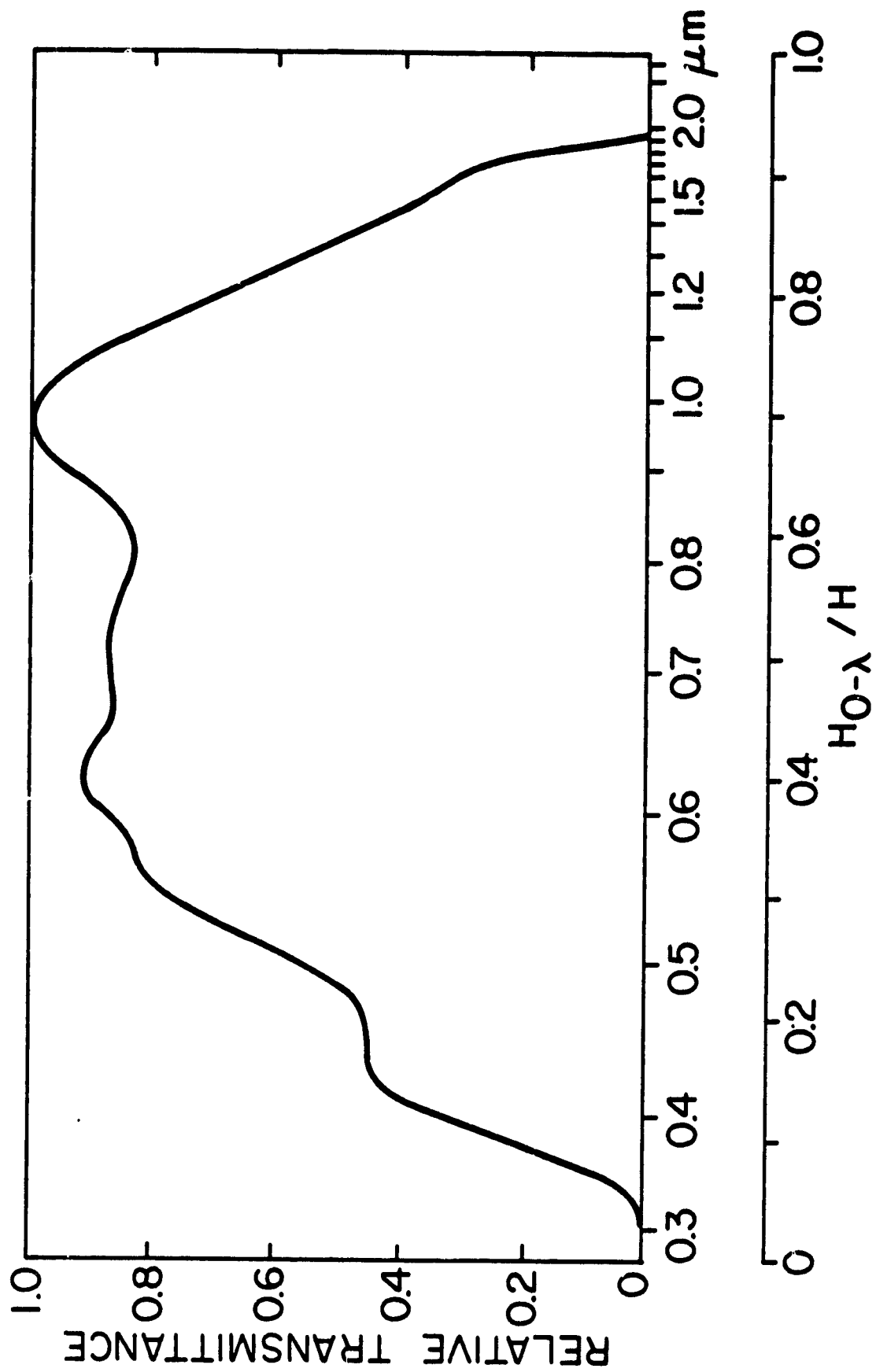


Figure 3

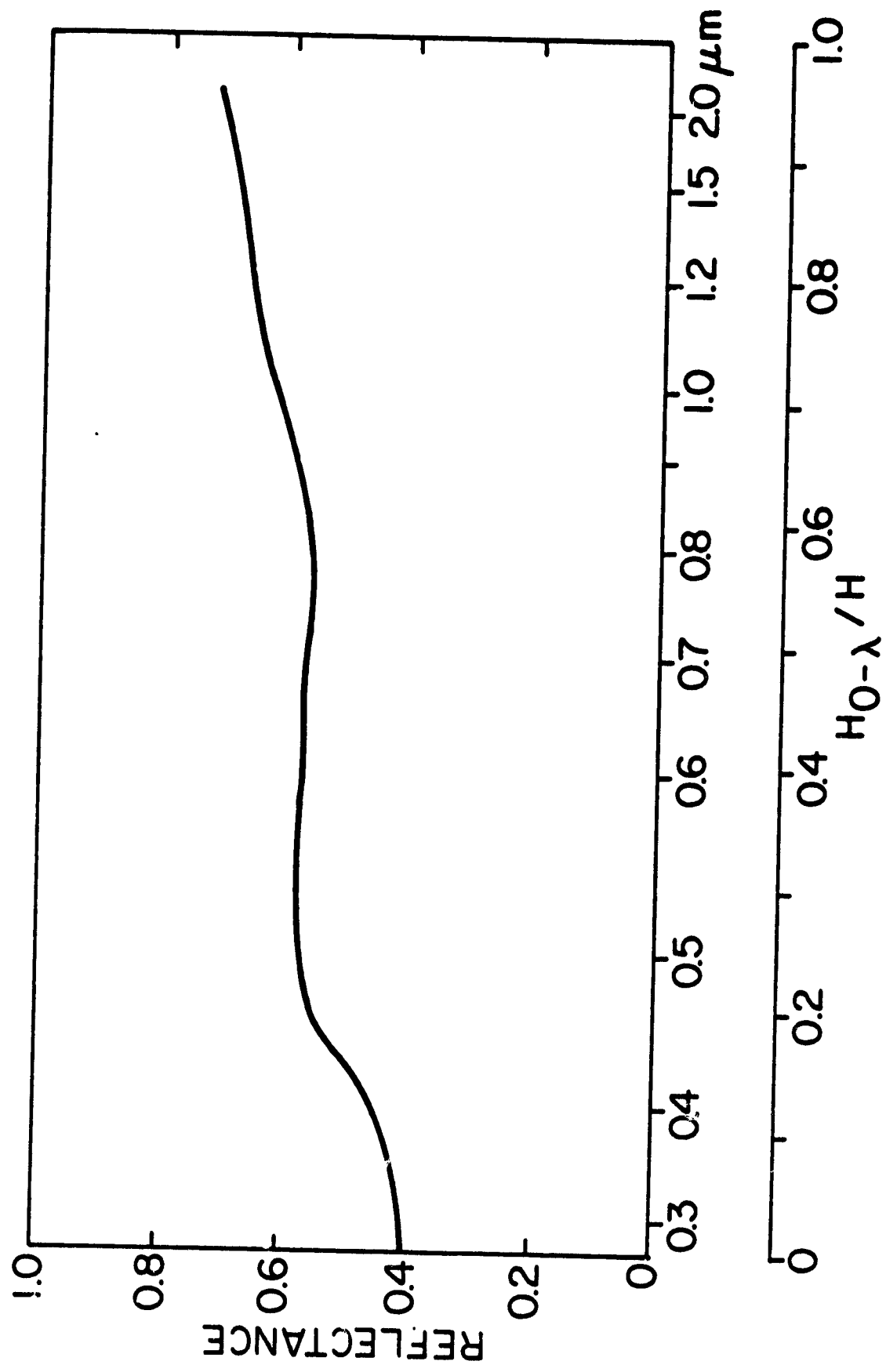


Figure 4

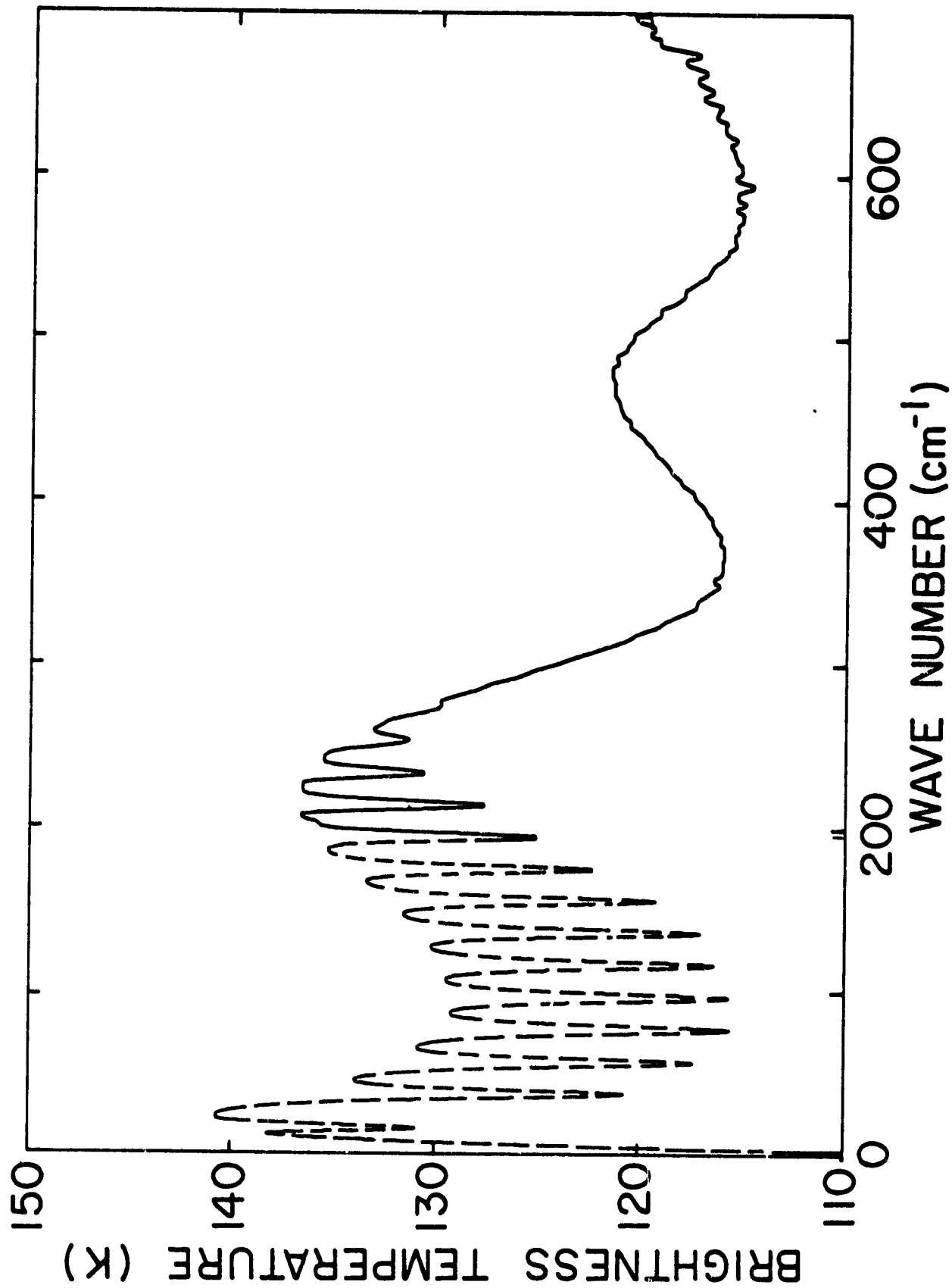


Figure 5

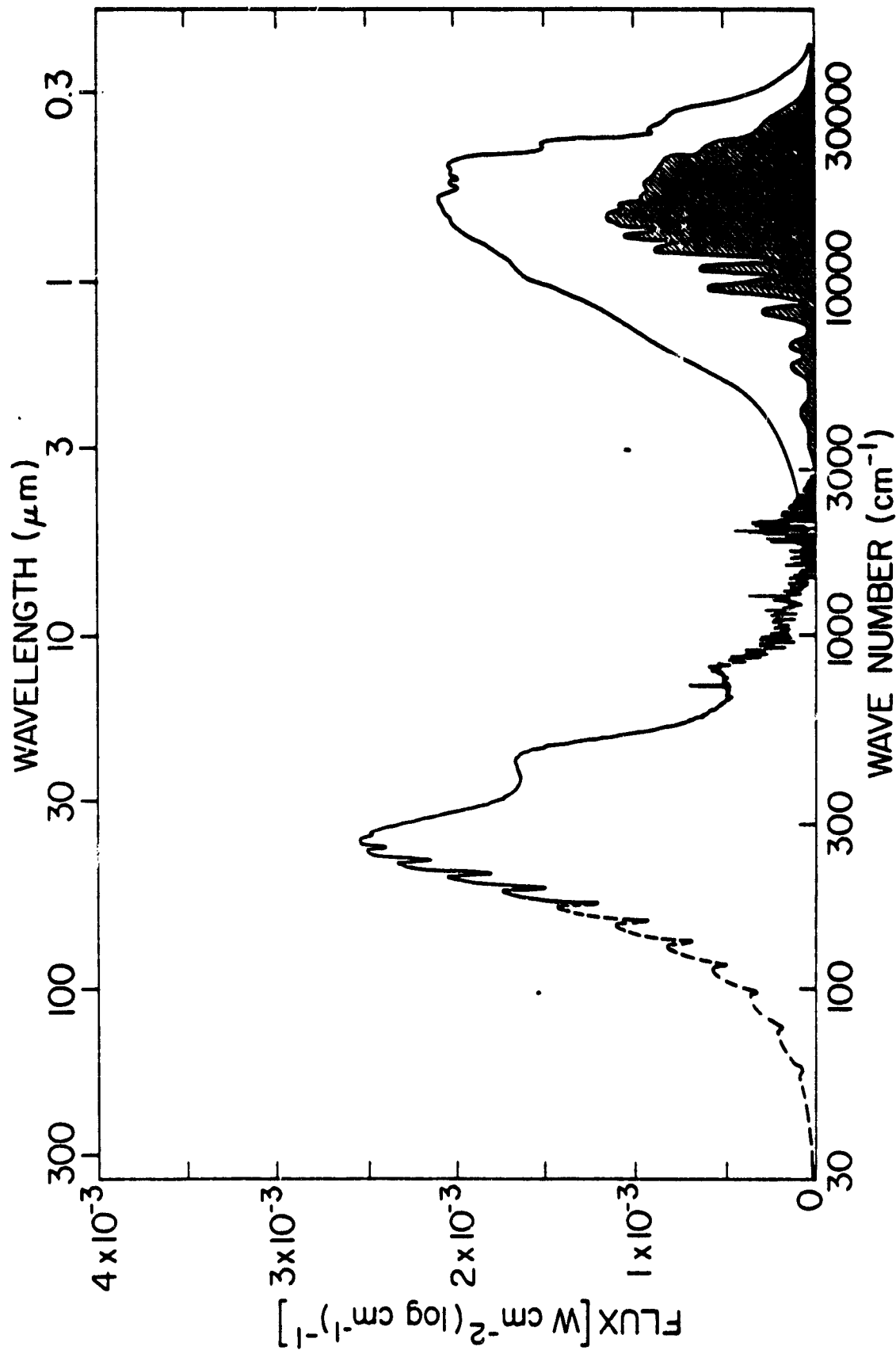


Figure 6